

Nonlocal failures in complex supply networks by single link *additions*

Dirk Witthaut¹ and Marc Timme^{1,2}

¹*Network Dynamics Group, Max Planck Institute for Dynamics and Self-Organization (MPI DS), D-37077 Göttingen, Germany*

²*Faculty of Physics, University of Göttingen, D-37077 Göttingen, Germany*

How do local topological changes affect the global operation and stability of complex supply networks? Studying supply networks on various levels of abstraction, we demonstrate that and how adding new links may not only promote but also degrade stable operation of a network. Intriguingly, the resulting overloads may emerge remotely from where such a link is added, thus resulting in nonlocal failure. We link this counter-intuitive phenomenon to Braess' paradox originally discovered in traffic networks. We use elementary network topologies to explain its underlying mechanism for different types of supply networks and find that it generically occurs across these systems. As an important consequence, upgrading supply networks such as communication networks, biological supply networks or power grids requires particular care because even *adding* only single connections may destabilize normal network operation and induce disturbances remotely from the location of structural change and even global cascades of failures.

PACS numbers: 89.75.-k, 89.20.-a, 88.80.hh, 05.45.Xt

I. INTRODUCTION

Stable operation of complex supply networks underlies the proper function of a broad range of biological and technical systems. For instance in plants, supply networks provide nutrients and water to cells in leaves and other plant parts [1]; the world wide web relies on stable information distribution [2]; and electric power grids operate only if electricity demand matches supply at every point of the grid [3, 4]. Whereas supply networks in biological systems are created during development and may be fixed after, e.g., leave damages, our technical infrastructure has to be constantly modernized and extended to meet technical developments and the future demand. One particular important example is the drastic change of electric power supply in the upcoming decades which provides an extraordinary challenge for the operation of future power grids [5–7]. New transmission lines have to be build in order to transport electric energy generated by wind turbines and other renewable energy sources to consumers at remote locations [8]. Due to the importance of a stable power supply and the enormous expenses of new transmission lines, a careful planning of the optimal future network topology is inevitable. This planning has to pay special regard to the *collective* dynamics of the complete network – an isolated stability analysis of single elements or local subnetworks is not sufficient [9–17]. A striking example highlighting the importance of collective effects in real supply networks is the power outage in western Europe on 4 November 2006. Here, the manual disconnection of one double-circuit power line in Northern Germany triggered power outages in many European countries up to Spain. A main reason for this fatal mis-planning was the inobservance of global effects beyond the local grid and the lack of communication between the different grid operators [18].

In this article, we analyze the collective response of

supply networks to the *addition* of new links and clarify a surprising, yet very general effect: We show that whereas additional links stabilize the operation of the network on average, specific potentially new links *decrease* the total network capacity and may deteriorate or even destroy network functionality. A similar effect in traffic flow was described and explained by Braess in a game theoretical framework [19, 20] and later confirmed experimentally and numerically in different systems [21–25]. Related phenomena were already discussed much earlier in [26, 27]. We explicate this counter-intuitive effect, referred to as Braess' paradox, for a range of model supply networks: an abstract messaging model, a flow model resembling Kirchhoff's laws for DC networks, a static power flow model and a dynamic oscillator model of AC power grids [4, 28]. Interestingly, adding certain links may not only cause cascading failures but also immediate overloads in parts of the network that are remote from the location of such links, thus indicating a non-local impact of specific link addition.

This article is structured as follows: After providing an intuitive explanation and a mathematical analysis of Braess' paradox for elementary model networks in Sec. II, we study different aspects of this effect in large complex networks. In Sec. III we show how the addition of new links can lead to a major breakdown of a supply network due to a cascading failure triggered by Braess' paradox. In complex networks, topological changes such as link addition and removal can cause severe nonlocal effects (Sec. IV). Finally we study in Sec. V which networks are susceptible to suffer Braess' paradox and which factors facilitate it. The first identification of Braess' paradox in oscillator networks has been briefly reported recently [29].

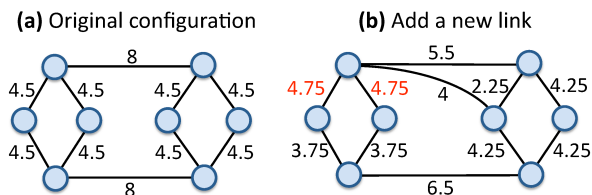


FIG. 1: (color online). Braess' paradox in an elementary messaging network. In one period, each node sends one message to each other node along the shortest path. The numbers specify the load F of each link. If a new link is added to the network (panel b), the load at two links adjacent to the new link *increases* from $F = 4.5$ to $F = 4.75$ (red numbers).

II. BRAESS' PARADOX IN ELEMENTARY NETWORK MODELS

We first reveal the mechanisms underlying Braess' paradox for small systems that allow a detailed analytic description. We demonstrate the importance of Braess' paradox in supply networks for four model classes: an abstract messaging model introduced by Motter and Lai [9], a DC power flow model, an AC power flow model and an oscillator model for power grid dynamics introduced by Filatrella *et al.* [28] for simple grids and extended to complex networks by Rohden *et al.* [4]. A detailed description of these models is provided in appendix A.

A. Braess' paradox in messaging networks

A simple model for supply networks was introduced by Motter and Lai [9] to study the dynamics of cascading failures. In this model every node sends one unit of the relevant quantity, e.g. information or electric energy, to each other node via the shortest path in the network.

A basic example for Braess' paradox in such a messaging network is shown in Fig. 1. The loads change when a new link is added. As expected, the total load is distributed over more links, such that the load decreases at most links (and on average). However, there are two edges of the network, where the load *increases* when the new edge is *added*. If the capacity of these links is limited to $K < K_c = 4.75$, they will become overloaded and drop out of service. This local failure may cause a breakdown of the complete network by a cascade of failures – an effect which will be studied in detail in Sec. III. This simple example already shows a basic mechanism which triggers Braess' paradox. When a new link is added, it can provide a shortcut for messages. This often increases the loads of some links *connecting* to the added one and these overloaded links, in turn, drop out of service (see also Sec. III).

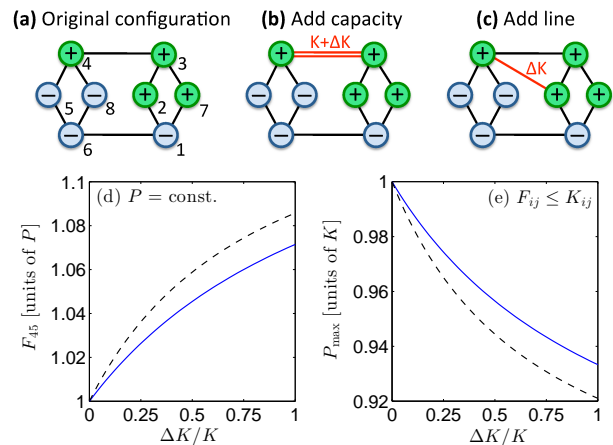


FIG. 2: (color online) Braess' paradox in a flow model. (a) Topology of the network. The vertices generate/consume the power $P_j = \pm P$. All edges have the same transmission capacity K . (b,c) Additional transmission capacity is provided by upgrading one link (b) or adding a new link (c). (d) Load of the link $4 \leftrightarrow 5$ as a function of the additional capacity if P is kept constant. (e) Maximum transmittable power P if the capacity of each link is limited as $F_{ij} \leq K_{ij}$. Results are shown for additional capacity (scenario (b), —) and an additional link (scenario (c), - - -).

B. Braess' paradox in flow networks

The messaging model briefly discussed above provides an elementary, well accessible model for supply networks, but relies on rather specific assumptions. Supply comes only in discrete units and is transported via the shortest paths, regardless of the capacity of the respective links. For general supply networks, more sophisticated models are needed.

Now, we first consider an elementary flow model which models, for instance, DC power grids or biological supply networks [1]. The network is specified by the transmission capacity $K_{ij} > 0$ between the nodes $i, j \in \{1, \dots, N\}$, where N denotes the number of nodes in the network. Obviously, we have $K_{ij} = K_{ji}$ and we set $K_{ij} = 0$ if no link exists between nodes i and j . Furthermore, each node of the network is characterized by the electric power P_j it generates ($P_j > 0$) or consumes ($P_j < 0$). We denote the flow from node i to node j by F_{ij} , which can be positive (power flows from i to j) or negative (power flows from j to i). The conservation of energy then reads

$$\sum_{j=1}^N F_{ij} = P_i \quad \text{for all } i \in \{1, \dots, N\}. \quad (1)$$

In general, this condition is not sufficient to uniquely fix the flows F_{ij} (see appendix A 2). We furthermore assume that the unique steady state is determined by the

condition that the total dissipated power

$$E_{\text{diss}} = \sum'_{i<j} \frac{F_{ij}^2}{2K_{ij}} \quad (2)$$

is minimal. Here, the primed sum runs over all existing links, i.e. all pairs (i, j) with $K_{ij} \neq 0$. For DC power grids these two conditions then imply Kirchhoff's circuit laws (see appendix A 2).

An elementary example for the occurrence of Braess' paradox in this flow model is shown in Fig. 2. The upper panels show the original network structure and two possible scenarios of upgrading the grid – either the capacity of the upper link is increased by an amount ΔK or another link with capacity ΔK is added. The remaining links have a capacity K and the nodes generate (+) or consume (–) the power P .

In the original network, a stable failure-free operation is possible as long as $P \leq P_{\text{max}} = K$. On the edge of the stability region, i.e. for $P = P_{\text{max}}$, the following six links are maximally loaded:

$$6 \leftrightarrow 1, \quad 1 \leftrightarrow 2, \quad 1 \leftrightarrow 7, \quad 3 \leftrightarrow 4, \quad 4 \leftrightarrow 5, \quad 8 \leftrightarrow 8.$$

If additional transmission capacity or a new link is added to the network as shown in Fig. 2 (b,c), the load of the adjacent links $F_{45} = F_{48}$ connecting to the new link increases as shown in Fig. 2 (d). Hence, these links are crucial for a failure-free operation of the complete network. If the original network is already operating close to the edge of the stability region, the addition of new capacity or a new link can damage the links $4 \leftrightarrow 5$ and $4 \leftrightarrow 8$ which may then trigger a power outage in the network. Therefore, the *increase* of local transmission capacity ΔK leads to a *decrease* of the maximum power P_{max} which can be transmitted through the network as shown in Fig. 2 (e). We note that P_{max} decreases monotonically with ΔK in this example of a linear flow networks whereas a different behaviour has been reported for traffic flow models [30].

The power flow in the elementary networks analyzed in Fig. 2 can be calculated analytically, which yields a closed condition for a failure-free operation of the supply network. In the following we consider the first scenario, where the capacity of the upper link $3 \leftrightarrow 4$ is increased by an amount ΔK . The condition of flow conservation (1) at each node gives rise to eight linear equalities for the eight non-zero flows F_{ij} . As one of the conditions is redundant, there is a one-dimensional family of solutions to the linear equations parametrized by a real number δ ,

$$\begin{aligned} (F_{16}, F_{21}, F_{32}, F_{43}, F_{54}, F_{65}) &= (F_a - \delta F_b), \quad \text{where} \\ F_a &= P(-1, -1, 0, +1, +1, 0) \\ F_b &= P(-2, -1, -1, +2, +1, +1). \end{aligned} \quad (3)$$

with

$$\begin{aligned} F_{71} &= F_{21}, & F_{37} &= F_{32}, \\ F_{84} &= F_{54} & \text{and} & F_{68} = F_{65}. \end{aligned} \quad (4)$$

due to the symmetry of the network. Minimizing the total dissipation (2) with respect to the parameter δ yields

$$\delta = \frac{\Delta K}{8K + 6\Delta K}, \quad (5)$$

such that the load of the critical links is given by

$$F_{54} = F_{84} = P \frac{8K + 7\Delta K}{8K + 6\Delta K}. \quad (6)$$

An overload occurs if the load is larger than the capacity of the link, i.e. if $|F_{54}| > K$. Thus we find that a failure-free operation of the supply network is only possible if

$$P \leq P_{\text{max}} = K \frac{8K + 6\Delta K}{8K + 7\Delta K}. \quad (7)$$

In particular, if the additional capacity ΔK increases, the maximum transferable power P_{max} decreases.

C. Braess' paradox in a AC power grid

Braess' paradox also occurs in AC power grids, which provide the backbone of our technical infrastructure [3, 31]. In this section we study the static operation of a grid in a power flow study before turning for a dynamic model in the following section. The details of the static flow model are described in appendix A 3.

As above we consider a power grid consisting of four generators and four identical consumers, cf. Fig. 3 (a), assuming a nominal grid voltage of 110 kV. One generator is chosen as slack node, while the remaining ones provide the fixed real power P_{gen} at the grid voltage such that $|U_{\text{gen}}| = 110 \text{ kV}$. Each consumer node consumes a fixed real power $P_{\text{con}} = -10 \text{ MW}$ and a reactive power $Q_{\text{con}} = -3.3 \text{ MVar}$. Hence, the power factor of the consumers is $\lambda = P_{\text{con}} / \sqrt{P_{\text{con}}^2 + Q_{\text{con}}^2} \approx 0.95$. We assume that the transmission lines are inductive and suffer from ohmic losses, setting $Z = (10 + 20i) \Omega$.

When the transmission line $2 \leftrightarrow 4$ is put into operation, this can cause Braess' paradox for the connecting lines. Figure 3 and Tab. I show the power loads in the network without (blue circle) and with (red squares) the new transmission line. The load of the connecting lines $4 \leftrightarrow 5$ and $4 \leftrightarrow 8$ *increases* by 8.5 %.

We remark that the effective loss in the network, i.e. the difference of the power generated and consumed at the nodes, will never increase when the new transmission line is put into operation. From this point of view, building new lines is always favorable. Still, the maximum power load of single links in the network can be *increased*, decreasing the margin to outage. In extreme situations, this may cause a shutdown of an overloaded transmission line and finally a cascade of failures leading to a major power outage.

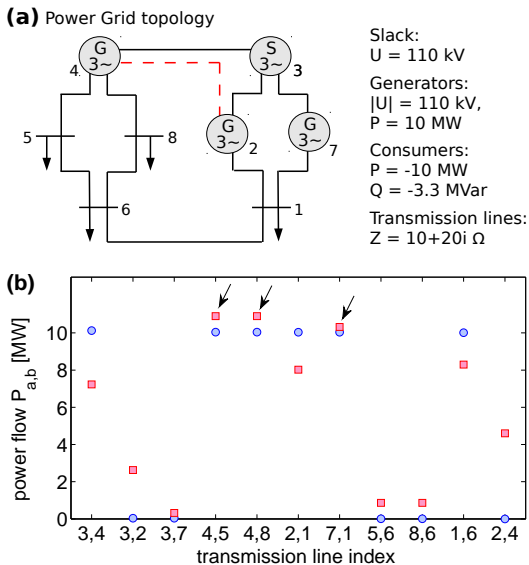


FIG. 3: (color online) Braess’ paradox in an AC power grid in static operation. (a) Network structure of the power grid including four consumers, three generators and a slack node. The detailed parameters are given in the text. (b) Power flow along each transmission line without (blue circles) and with the additional line (red squares). The transmission lines marked by an arrow are subject to Braess’ paradox: The maximum load $P_{4,5} = P_{4,8}$ and $P_{7,1}$ increase when the new line is added to the power grid. The actual load of several transmission lines is given in Tab. I.

| | initial grid | with additional line |
|---------------------|--------------|----------------------|
| P_{slack} | 10.191 MW | 10.175 MW |
| $P_{4,5} = P_{4,8}$ | 10.04 MW | 10.90 MW |
| $P_{3,4}$ | 10.12 MW | 7.23 MW |
| $P_{2,4}$ | 0 MW | 4.60 MW |

TABLE I: Power generation and load of selected transmission lines for the power grid shown in Fig. 3.

D. Braess’ paradox and desynchronization in oscillator networks

As demonstrated recently [29], Braess’ paradox also exists in oscillator networks. In particular, networks of two-variable oscillators describing the *dynamics* of AC power grids and thus going beyond the static regime analyzed so far, typically exhibit Braess paradox for at least a fraction of (potentially) added links. The class of oscillator models [4, 28] is particularly appealing as it captures several collective phenomena present in real power grids whereas it is simple enough to admit a mechanistic understanding of such phenomena and simulations also for large complex networks.

In this model, both generators and consumers are assumed to be synchronous machines and thus obey the same equation of motion with a parameter P giving the generated ($P > 0$) or consumed ($P < 0$) power. The

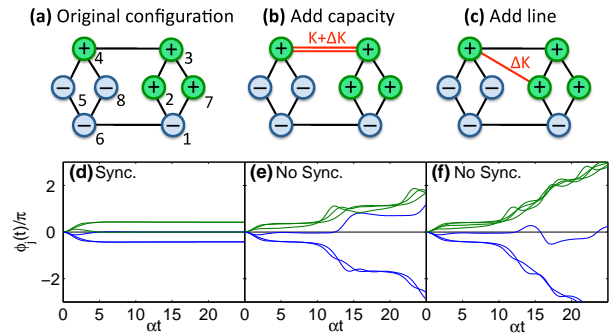


FIG. 4: (color online) Braess’ paradox in an oscillator model [29] (a-c), Topology of the network. The vertices generate/consume the power $P_j = \pm P$. The transmission lines have a capacity K . (d) The original network converges to a phase-locked state. When the capacity of one link is doubled (e), or when a new link is added to the network (f), the steady state ceases to exist and phase synchronization breaks down. Parameters are $K = 1.03 P$, $\Delta K = K$, $\alpha = P$, and the initial conditions are $\phi_j = \dot{\phi}_j = 0$.

state of each machine is determined by its phase angle $\theta(t)$ and velocity $\dot{\theta}(t)$. The mechanical phase of the j th machine is written as $\theta_j(t) = \omega_0 t + \phi_j(t)$, where $\omega_0 = 2\pi \times 50 \text{ s}^{-1}$ or $\omega_0 = 2\pi \times 60 \text{ s}^{-1}$ is the reference frequency of the power grid. The equation of motion is obtained via the principle of energy conservation, that is the generated or consumed power of each element must equal the power exchanged with the grid plus the accumulated and the dissipated power. The power transmitted between machines i and j is proportional to the sine of the phase difference and the capacity of the transmission line K_{ij} . As shown in detail in appendix A 4, the equations of motion for the phase differences then read

$$\frac{d^2 \phi_j}{dt^2} = P_j - \alpha \frac{d\phi_j}{dt} + \sum_i K_{ij} \sin(\phi_i - \phi_j). \quad (8)$$

Again we first consider an analytically solvable model network which is similar to the ones discussed in the previous sections (cf. Fig. 4). Four generators with $P_j = +P$ and four consumers with $P_j = -P$ are connected by transmission lines with capacity K . A stable steady state exists for the original network structure (Fig. 4 (a)), if the power is smaller than a critical value

$$P \leq P_{\text{max}} = K, \quad (9)$$

and the system rapidly relaxes to this phase-locked state of partial synchrony, cf. Fig. 4 (d). As in the previous examples, the increase of the transmission capacity or the addition of a new link can induce Braess’ paradox. In these cases synchronization becomes impossible – the phases $\phi_j(t)$ cannot phase lock as shown in Fig. 4 (e,f). For a real power grid this effect would imply the automatic shutdown of the desynchronized generators, which may then cause a major power outage in the complete network.

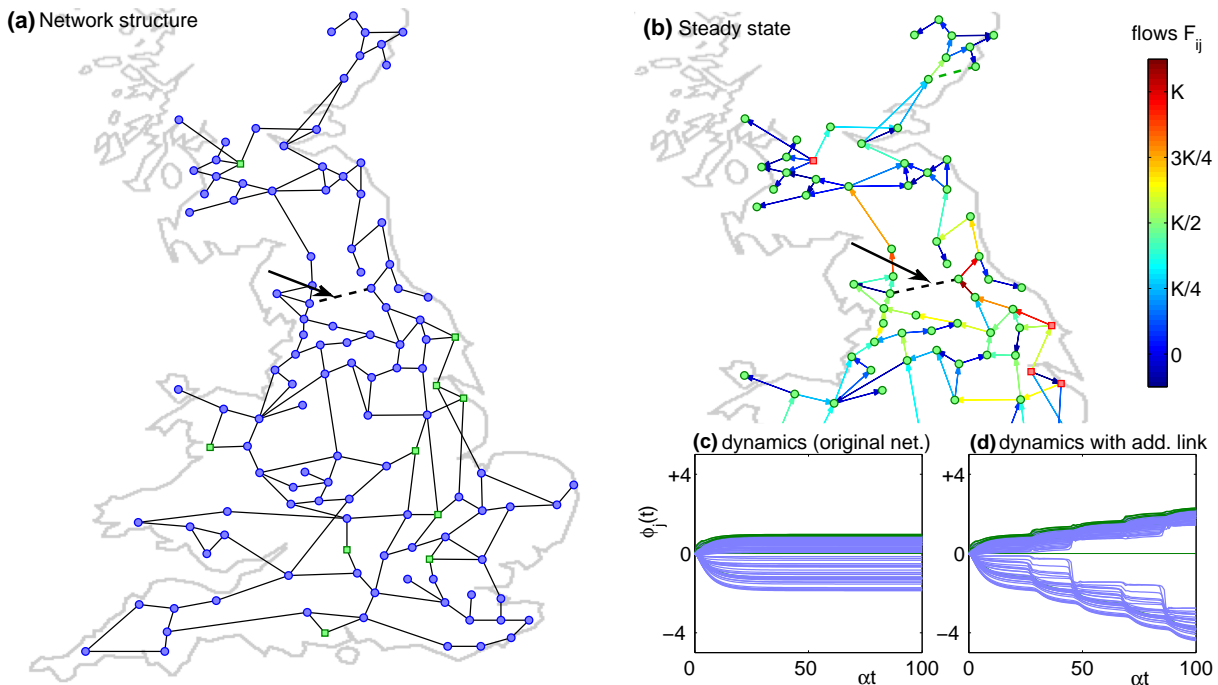


FIG. 5: Desynchronization due to Braess' paradox in an oscillatory power grid with complex topology [29]. (a) Topology of the British power grid, consisting of 120 nodes and 165 transmission lines (thin black lines) [12]. Ten nodes are randomly selected to be generators ($P_j = 11P_0$, \square), the others are consumers ($P_j = -P_0$, \circ). The dashed new link causes desynchronization due to Braess' paradox. (b) Power flow in the original network for $K = 13P_0$. The load of several transmission lines in the neighborhood of the new link is already close to the maximum capacity K . (c) For $K = 13P_0$ and $\alpha = P_0$, the initial network converges to a phase-locked steady state. (d) Synchronization becomes impossible after the new link has been added. The initial condition is fully synchrony, $\phi_j = \dot{\phi}_j = 0$.

The loss of synchrony in an oscillator network due to Braess' paradox is a rather subtle effect. The condition for the existence of a phase-locked steady state in the power grid model $\phi_j = \dot{\phi}_j = 0$ is equivalent to the conservation of the flow

$$\sum_{j=1}^N F_{ij} = P_i \quad \forall i = 1, \dots, N_n. \quad (10)$$

For the oscillator model, the power flows are given by

$$F_{ij} = K_{ij} \sin(\phi_j - \phi_i). \quad (11)$$

Therefore, we can divide the condition for the existence of a phase-locked steady state into a dynamic and a geometric component. In addition to the conservation of the flow (10) we have to satisfy a geometric condition: For every cyclic path in the network, the sum of all phase differences must vanish such that all phases are well-defined,

$$\sum' (\phi_j - \phi_i) = \sum' \arcsin(F_{ji}/K_{ji}) = 0 \pmod{2\pi}. \quad (12)$$

The prime indicates that the sum is taken along a cyclic path. For the networks shown in Fig. 4 one can easily find values F_{ij} which satisfy flow conservation, cf. Eq. (3), but the condition (12) is no longer fulfilled. For such F_{ij} 's, despite the fact that all dynamical conditions (10) are

satisfied, no steady state exists due to *geometric frustration*, the incapability of the system to satisfy (12) along all cycles of the network. In fact, the critical coupling strength K_c for the existence of a phase-locked state is increased. Thus geometric frustration limits the capability of the network to support a steady state.

Braess' paradox in oscillator networks is rooted in the geometric frustration of small cycles, which are generally present in most complex networks [29]. We speculate that condition (12) is more often satisfied along long cycles because these have a larger number of variables, i.e. the restriction can be "solved" in higher-dimensional space of phase differences. Braess' paradox occurs in many, but not all complex networks as elementary cycles are typically overlapping such that the effects of geometric frustration depend on the precise network topology and are as such hard to predict.

As an important example, we consider the British high-voltage power transmission grid shown in Fig. 5, cf. [12]. In our study, we randomly choose ten out of 120 nodes to be generators ($P_j = +11P_0$), while the remaining ones are consumers ($P_j = -P_0$). For $K = 13P_0$ the original network relaxes to a phase-locked steady state as shown in part (c) of the figure. If one inappropriate new link is added (dashed black line), global synchronization (phase locking) is lost due to Braess' paradox for the given cou-

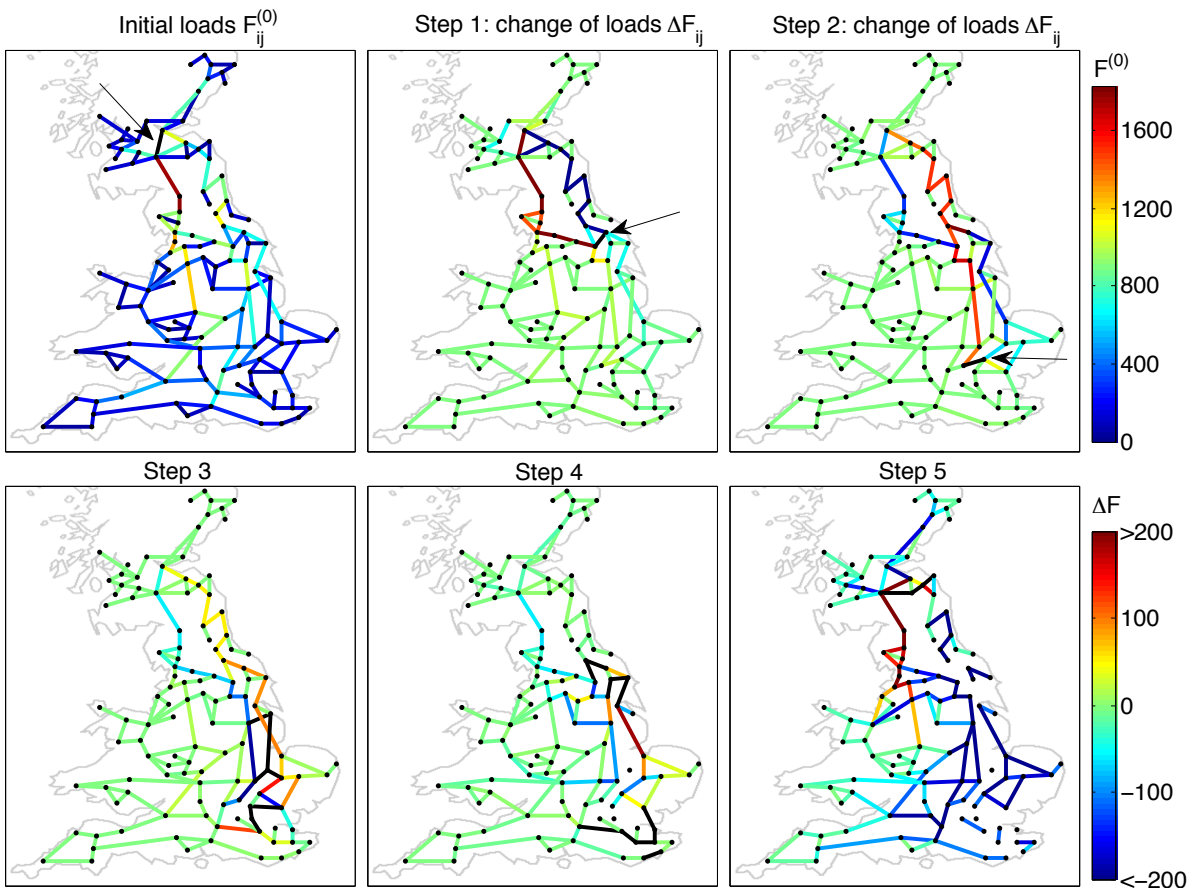


FIG. 6: A cascading failure triggered by the addition of a new link in the messaging model. Upper left panel: The initial network and the loads $F_{ij}^{(0)}$ of all links in a color code. The link colored in black is added to the network. The remaining panels show how the failure propagates through the network. The color code gives the change of the load ΔF in comparison to the previous step. Links colored in black are overloaded and drop out of service. Note that in this example links are overloaded which are *not* nearest neighbors of the additional link which triggers the cascading failure. These links are marked by arrows in step 1 and 2. In this simulation we have used the coarse grained structure of the British power grid with 120 nodes and 165 edges as described in [12]. The tolerance parameter is $\alpha = 0.32$.

pling strength K . Instead, the power grid decomposes into two asynchronous fragments as shown in part (d) of the figure.

Furthermore, this example emphasizes the importance of the lines connecting to the newly added one: These lines may easily become overloaded when the new edge is added to the network, finally causing a system wide failure. In particular, also lines indirectly connecting to the newly added one may be affected in a similar way. Figure 5 (b) shows the power flow in the steady state before the new link is added. One observes that several transmission lines in the neighborhood of the new link are heavily loaded. These lines get overloaded when the new link is put into operation, causing the desynchronization of the grid. Generally, adding new transmission lines are assumed to most strongly change the load distribution in the network if they are build in regions where the existing lines are already heavily loaded. In fact, loads are often thought to be reduced due to the new line. However,

load redistribution is not necessarily supportive, as shown above. For more details on the physics of Braess' paradox in oscillator networks, see also [29].

III. CASCADING FAILURES TRIGGERED BY THE ADDITION OF LINKS

The messaging model studied in Sec. II A was initially introduced to study how the damage of a *single* link can induce a major failure in large parts of the grid [9, 12]. This scenario is very important for real supply networks, in particular for power grids, as most major power outages are the result of a cascade of failures. A prominent example is the power outage in the western European power grid on November 4th 2006, which was triggered by the shutdown of one double-circuit transmission lines over the river Ems in north-western Germany [18]. As a consequence ten million households were disconnected

from the power supply. Power outages even occurred in Spain, approximately 2000 km away from the cause of the cascading failure. In this section we show that not only the removal or damage of at single transmission line, but also the *addition* of a new transmission line can cause a cascading failure due to Braess' paradox.

An example for a cascading failure by link addition is shown in Fig. 6. Again, we consider the coarse grained structure of the British power grid with 120 nodes and 165 link [12]. The upper left panel shows the load $F_{ij}^{(0)}$ of each link of the initial network in a colormap plot. As in the original model [9], we assume that the capacity of each link is adapted to the loads

$$K_{ij} = (1 + \alpha)F_{ij}^{(0)} \quad (13)$$

with a tolerance parameter $\alpha \geq 0$. If the load F_{ij} exceeds the capacity K_{ij} , then the link becomes overloaded and drops out of service, i.e. it is removed from the network.

Now we consider the effect of the *addition* of a new link to the network. The new link is colored in black and marked by an arrow in in the upper left panel of Fig. 6. We assume that the new link has a rather high capacity $K_{\text{new}} = \max_{ij}(K_{ij})$. The upper middle panel then shows how the loads of all links changes after the addition of this link. As expected from the study of the elementary model in Sec. II A, the load of the *connecting lines* along the western coast increases. For $\alpha = 0.32$, only a single link becomes overloaded which is colored in black and marked by an arrow. This failure then again causes a redistribution of the loads in the network and the overload of another link. This finally triggers a whole cascade of failure as shown in the remaining panels of Fig. 6. After six steps, the cascade stops and the network is decomposed into 13 different components. The largest component includes 85 nodes, while 6 nodes are completely disconnected.

An important question is how crucial the addition of a new link is in general, in particular in comparison to the removal of a single links. To answer this question, we have simulated the impact of cascading failures as a function of the tolerance parameter α for the coarse grained structure of the British power grid. A single link is added or removed at random positions in the network and we analyze the final structure of the network after the cascade of failures has come to an end. Figure 7 shows the size of the largest connected component G relative to the size of the initial network. The simulations reveal a surprising result: Link addition has even more severe consequences than link removal in the sense that it leads to smaller values of G/G_0 . However, this effect is partly due the fact that links are added at completely random positions such that they generally connect *distant* areas of the network. Obviously, this can have a stronger effect on the network flow than the 'local' removal of a link. The addition of links at random positions is also rather unrealistic. Thus we also consider an alternative scenario where links can be added only between nodes with a distance of two. The numerical results (Fig. 7,

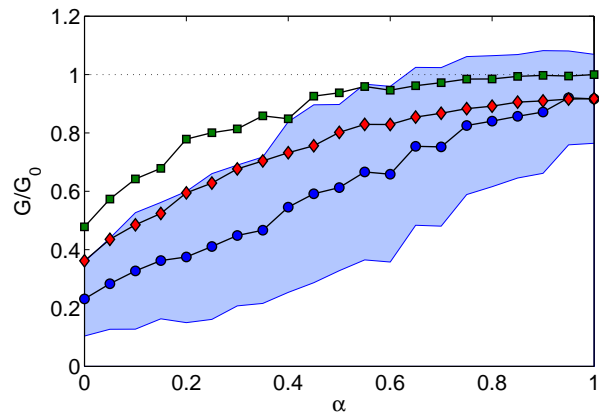


FIG. 7: (color online) How harmful are single link changes? Characterization of the final state after a cascading failure in the messaging model. Plotted is the relative size of the largest connected component G/G_0 in the final state, i.e. the final size divided by the initial size as a function of the tolerance parameter α . We consider the addition of links at random positions (blue circles), the addition of links at local position (green squares) and the removal of links (red diamonds). Local position means that a link is added between two random nodes with initial graph distance of 2. In this simulation we have used the coarse grained structure of the British power grid with 120 nodes and 165 edges as described in [12]. Results have been averaged over 200 random positions (for local and global random addition of links) and over all 165 existing links (removal of links). The shaded (blue) area shows the standard deviation for the cases of link addition at random position.

green squares) reveal that such a local addition of links has a less severe effect than the removal of links, but both can be substantial.

IV. NONLOCAL IMPACT OF LINK ADDITION AND REMOVAL

Cascading failure events such as those illustrated in Fig. 6 highlight that a single link addition may induce strong nonlocal impacts. In the example (Fig. 6), the cascade is triggered by the addition of a link in Scotland. The load of the connecting links is strongly modified, also beyond the immediate neighborhood of the novel link. In particular, a rather weak link located in northeastern England becomes overloaded, while the links in the immediate neighborhood remain in operation. In the second step, one link at an even further distance becomes overloaded. Finally, several nodes in southeastern England are fully disconnected from the network – nodes which are far away from the link which caused the failure.

The example shown in Fig. 6 is surely extreme, but a strong nonlocal impact triggered by changes of the network topology is by no means exceptional: To analyze the geographic properties of cascading failures quantitatively, we calculate the distance between the overloaded

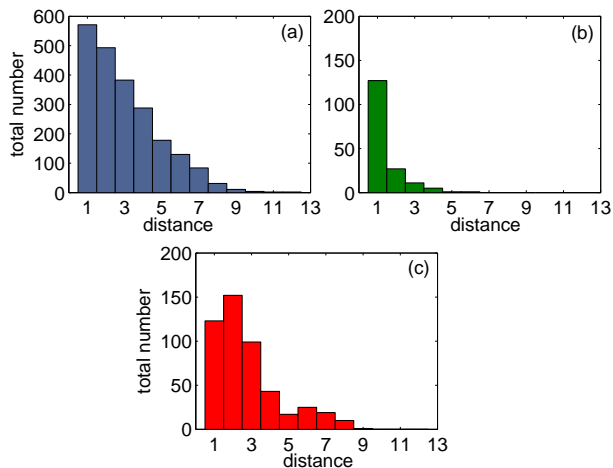


FIG. 8: Nonlocal impact of link addition and removal (here: in the messaging model). (a-c) Histograms of the distances of the initially added/removed link to the links which become overloaded the first step. We consider (a) the addition of links at random positions, (b) the addition of links at local position and (c) the removal of links. Note that the distance is defined in terms of the original unmodified network in the case of link removal. For link addition, distance is defined in terms of the modified network, i.e. the network including the additional link. In this simulation we have used the coarse grained structure of the British power grid with 120 nodes and 165 edges as described in [12]. Results have been collected for 200 random positions.

links and the added/removed link, which causes the overload. Figure 8 shows a histogram of these distance for the first step of the cascade. As above, we consider three scenarios: (a) the addition of a link at a random position, (b) the local addition of a link and (c) the removal of a link. For scenarios (a) and (c) it is observed that overloads frequently occur at remote positions. In the case of link removal, the next-to-nearest neighbors are even more vulnerable to an overload than the nearest neighbors. If link addition is restricted to a local position (scenario b), then also the immediate impact occurs predominantly at local positions. However, the dynamic consequences often reach beyond the local neighborhood in the network. Already in the second step of the cascade (not shown), almost no differences can be observed between the three different scenarios.

We note that these findings do not contradict the claim that the connecting lines are crucial for the possibility of Braess' paradox. They rather show that we have to consider the connecting lines beyond the immediate neighborhood, too. In particular, in the example studied in Fig. 6, one can identify a rather long path of connecting lines, whose load strongly increases after the addition of the new link (the red link in the upper middle panel in Fig. 6). The overload then occurs on the weakest of these links, not on the nearest.

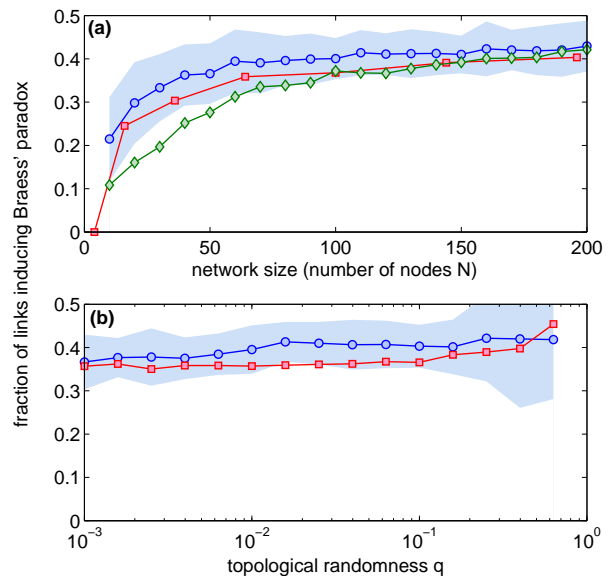


FIG. 9: (color online) Prevalence of Braess' paradox across different topologies: Randomized ring lattices (blue circles, [32]), randomized square lattices (red squares, [33]) and networks with algebraic degree distribution (green diamonds, [34]). Plotted is the fraction of links whose removal leads to a *decrease* of the maximum flow F_{\max} as a function of (a) the network size ($q = 0.1$) and (b) the topological randomness of the network ($N = 200$). The shaded blue area shows the standard deviation for the randomized ring lattices. Solid lines are drawn to guide the eye. Random networks which are not globally connected were discarded, in particular there is no data point at $q = 1$ as random networks with average degree $d = 4$ are almost always disconnected.

V. BRAESS' PARADOX ON COMPLEX NETWORK TOPOLOGIES

Braess' paradox arises for different models of supply networks and can have severe consequences for the operation of the network. We now show that in large complex networks this phenomenon is the rule rather than the exception. We systematically study the occurrence of Braess' paradox for the flow model introduced in Sec. II B and analyze how this behavior depends on the size and topology of the network.

To analyze how topological changes impact network dynamics for different classes of random networks, we first consider classes of networks that interpolate between regular and random topology, also referred to as small-world networks [32, 33]. Starting with a ring lattice where each node is connected to its nearest and next-to-nearest neighbors or a square lattice, every link is rewired with probability q , i.e. removed and re-inserted at a different randomly chosen position. Furthermore we consider networks with an algebraic degree distribution generated by random preferential attachment [34]. The average degree is $d = 4$ for the randomized lattices and $d = 4 - 4/N \approx 4$ for the algebraic network. In each case, half of the nodes

are randomly chosen to be generators ($P_j = +P_0$) or consumers ($P_j = -P_0$).

We then check for each link how its removal affects the maximum flow $F_{\max} = \max_{ij} |F_{ij}|$ in the network. A link is said to induce Braess' paradox if F_{\max} decreases after the removal. This definition is exactly the same as above as the re-addition of the link would increase F_{\max} which could then cause a fatal overload. For each random network we count the number of links which induce Braess' paradox and average over one-hundred realizations of the network structure. We then analyze how this number depends on the size and topology of the networks.

The numerical results plotted in Fig. 9 demonstrate that Braess' paradox is common in complex flow networks. For large networks with 200 nodes, more than 40 % of the links impede the operation of the the supply network in the way that their removal is beneficial as it decreases the maximum load F_{\max} . However, the impact of a single link decreases with the total number of links present in the network. Therefore, the magnitude of the change of F_{\max} is generally smaller for larger networks, see Fig. 10 (b) where we have plotted a histogram for the difference of the maximum loads before and after the link removal

$$\Delta F_{\max} = F_{\max, \text{after}} - F_{\max, \text{before}}. \quad (14)$$

for a small ($N = 16$) and a large ($N = 196$) network. One clearly sees that the probability for large changes ΔF_{\max} is extremely small for the larger network.

Furthermore, Braess' paradox prevails across all types of network topologies and model dynamics considered here. For large networks, the topology has only a minor influence on the probability that a link induces Braess' paradox. Even more, the probability is almost independent of the topological randomness q as shown in Fig. 9 (b). However, topological changes have a more severe impact in networks with a regular topology as shown in Fig. 10 (a), where we compare the difference of the maximum flow ΔF_{\max} before and after links removal for a randomized square lattice with $q = 0.005$ (close to regular) and $q = 0.5$ (close to random). The probability for large values of F_{\max} is much larger for the regular network with $q = 0.005$.

In conclusion we find that the probability to observe Braess' paradox is almost independent of the of the network topology and increases with the network size. However, the impact of a single link is largest for regular structures and decreases with the network size. This finding is consistent with the results for oscillator networks discussed in [29].

VI. DISCUSSION

We have revealed and analyzed Braess' paradox for different models of supply networks: Against the naive intuition, the addition of new connections in a network does *not* always increase the overall transmission capacity of

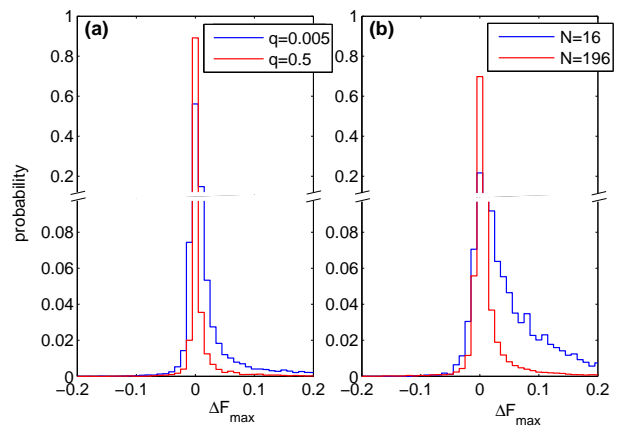


FIG. 10: (color online) Impact of link removal on the maximum flow in a supply network. Histogram displays the difference of the maximum flow ΔF_{\max} before and after link removal (14) for randomized square lattices [33] with (a) $N = 100$ and two different values of q and (b) $q = 0.1$ and two different values of N . A negative difference ΔF_{\max} indicates Braess' paradox.

the network. An elementary model system was designed to analytically study this paradoxical behavior, while numerical simulations have revealed that a substantial fraction of potential links induce this deleterious transition. Furthermore, we have shown that catastrophic failures of complex supply networks may not only be caused by failures of single elements or links but also by the addition of *single* links. In particular, networks may destabilize due to a non-local overload.

Future model studies must include the detailed structure of supply networks as well as the spatial and temporal heterogeneity of generation and demand. For instance, both the consumption and generation of electric energy in modern power grids is strongly fluctuating. This notwithstanding, Braess' paradox is a general feature such that it can play a crucial role in real supply networks. In the future, it will be of great scientific as well as economic interest to understand how these phenomena depend on the topologies of the underlying networks in detail, cf. [15, 35–37]. In particular, a badly designed electric power grid subject to Braess' paradox may cause enormous costs for new but counterproductive electric power lines that actually reduce grid performance and stability.

While Braess' paradox has been observed in real-world traffic networks in several locations [21–25], its effects are less apparent for different types of supply networks. For instance, power grids are usually operated far from their load limit such that local structural changes do not cause obvious global failures. However, periods of extreme load do occur and are expected to become more likely in future power grids with many strongly fluctuating renewable energy sources. In such a period of extreme load, small local changes of the network structure may cause a global breakdown. For instance, there was a

significant East-West power flows in the European power grid on 4 November 2006 because of a large wind feed-in in Germany. In this situation, the disconnection of one double-circuit transmission line in Northern Germany was sufficient to trigger a global power outage in most of Western Europe [18]. A key result of this work is that in such a situation the *addition* of a new link can be just as fatal as the disconnection of an existing one.

Acknowledgments

We thank S. Grosskinsky, M. Rohden, A. Sorge, D. Heide, and R. Sollacher for valuable discussions. Supported by the Federal Ministry of Education and Research (BMBF) Germany under grant number 01GQ1005B and by a grant of the Max Planck Society to M.T.

Appendix A: Models of supply networks

In this appendix we provide a detailed description of the different models of supply networks used in the present paper.

1. Messaging model

A popular model to study the stability of supply and communication networks, in particular the vulnerability to cascading failures, has been introduced by Motter and Lai [9]. In contrast to the original study we focus on the links in the network, not the nodes. In particular, we assume that a link drops out of service if it is overloaded, while the nodes are not affected.

The messaging model assumes that at each time step, one unit of information or energy is sent from each node to each other node in the connected component along the shortest path. The load of each link F_{ij} is then given by the number of shortest paths running over this link $i \leftrightarrow j$, which is nothing than the edge betweenness centrality. Furthermore, it is assumed, that the capacity of each link proportional to the load of the link in the initial intact network,

$$K_{ij} = (1 + \alpha)F_{ij}^{(0)}. \quad (\text{A1})$$

Here, the superscript (0) denotes the intact network. Then Motter and Lai analyze what happens if one link is damaged. Obviously the other links have to take over the load such that F_{ij} will generally increase. If the load exceeds the capacity of a link, $F_{ij} > K_{ij}$, then this link will also drop out of service, which can trigger a cascade of failures disconnecting the entire grid.

2. Flow model

One of the simplest models of supply networks considers only the flow between different elements of the network. A similar model has also been used to model biological flow models in [1]. The power grid is specified by the transmission capacity $K_{ij} > 0$ between the nodes $i, j \in \{1, \dots, N\}$, where N denotes the number of nodes in the network. Obviously, we have $K_{ij} = K_{ji}$ and we set $K_{ij} = 0$ if no link exists between nodes i and j . Furthermore, each node of the network is characterized by the electric power P_j it generates ($P_j > 0$) or consumes ($P_j < 0$).

We denote the flow from node i to node j by F_{ij} , which can be positive (power flows from i to j) or negative (power flows from j to i). The conservation of energy then directly leads to the condition

$$\sum_{j=1}^N F_{ij} = P_i \quad \text{for all } i \in \{1, \dots, N\}. \quad (\text{A2})$$

In general, energy conservation is not sufficient to uniquely fix the flows, as it poses only $N - 1$ linearly independent constraints for the L independent non-zero variables F_{ij} , L being the number of links in the network.

The unique steady state is determined by the condition that the total dissipated power

$$E_{\text{diss}} = \sum'_{i < j} \frac{F_{ij}^2}{2K_{ij}} \quad (\text{A3})$$

should be minimal. In this expression, the primed sum runs only over existing transmission lines, i.e. only over links with $K_{ij} \neq 0$. To minimize this expression respecting the conservation of energy, we use the method of Lagrangian multipliers, i.e. we minimize

$$\begin{aligned} L &= \sum_{i < j} \frac{F_{ij}^2}{2K_{ij}} - \sum_i \lambda_i \left(\sum_j F_{ij} - P_i \right) \\ &= \sum_{i < j} \left(\frac{F_{ij}^2}{2K_{ij}} - (\lambda_i - \lambda_j)F_{ij} \right). \end{aligned} \quad (\text{A4})$$

Minimization yields the condition

$$\begin{aligned} \frac{\partial L}{\partial F_{ij}} &= K_{ij}^{-1}F_{ij} - (\lambda_i - \lambda_j) \stackrel{!}{=} 0 \\ \Rightarrow F_{ij} &= K_{ij}(\lambda_i - \lambda_j) \end{aligned} \quad (\text{A5})$$

Thus, the flow from i to j is given by a potential difference $\lambda_i - \lambda_j$ multiplied by the transmission capacity K_{ij} . Substituting this result into equation (A2), we find that the potential is determined by a linear system of equations

$$\sum_j K_{ij}(\lambda_i - \lambda_j) = P_i. \quad (\text{A6})$$

for convenience, we rewrite this system of equations in a vectorial form

$$\tilde{K}\vec{\lambda} = -\vec{P} \quad (\text{A7})$$

where we have defined the matrix elements

$$\tilde{K}_{ij} = K_{ij} - \left(\sum_k K_{ik}\right)\delta_{ij} \quad (\text{A8})$$

and the vectors \vec{P} and $\vec{\lambda}$ collect the values of the power generated/consumed in each node P_j and the potentials λ_j .

We note that the oscillator model (A17) reduces to this model in the steady state, when the phase differences are so small that one can approximate $\sin(\phi_i - \phi_j) \approx \phi_i - \phi_j$, which is typically the case if the couplings K_{ij} are very large. The power flow model can thus be seen as a limiting case of the oscillator model.

3. Static flow in AC power grids

In an AC power grid, one has to take into account that not only real but also reactive power is transmitted via the network. Each link of the grid is characterized by its complex impedance, not just its maximum transmission capacity. In a static power flow study one calculates the voltage of each node such that the electric power is conserved at each node [31].

Every node a is characterized by its voltage U_a compared to the ground. A transmission line between the nodes a and b carries the current

$$I_{a,b} = \frac{1}{Z_{a,b}}(U_a - U_b), \quad (\text{A9})$$

where $Z_{a,b}$ is the impedance of the line. The electric power transmitted from or to a node of the network is then given by

$$S_a = \sum_b S_{a,b} = \sum_b 3U_a I_{a,b}^*, \quad (\text{A10})$$

where the star denotes complex conjugation. The real part gives the real transmitted power P_a , while the imaginary part Q_a is the reactive power,

$$S_a = P_a + iQ_a. \quad (\text{A11})$$

Power conservation requires that the total transmitted power equals the power generated or consumed at the respective node:

$$S_a = S_{a,\text{source}}. \quad (\text{A12})$$

In our study we distinguish three types of nodes; generators, consumers and a slack node. Every node imposes two conditions depending on its type:

- *Generator* nodes have a fixed nominal voltage and provide a fixed real power:

$$P_a \stackrel{!}{=} P_{a,\text{source}}, \quad |U_a| \stackrel{!}{=} |U_{a,\text{source}}|.$$

- *Consumers* are defined by fixed values of the real and reactive power:

$$P_a \stackrel{!}{=} P_{a,\text{source}}, \quad Q_a \stackrel{!}{=} Q_{a,\text{source}}.$$

- Furthermore, one introduces a *slack node* which is an ideal voltage source with the nominal voltage of the grid, i.e. the magnitude and the phase of the voltage are fixed:

$$U_a \stackrel{!}{=} U_{a,\text{source}}.$$

The slack node compensates any unbalanced real or reactive power in the network.

In a power grid with N elements, one thus has to solve $2N$ algebraic nonlinear equations for the $2N$ free variables $\Re(U_a)$, $\Im(U_a)$, $a \in \{1, \dots, N\}$. Given the voltages U_a one can easily calculate the power flows $S_{a,b}$ via Eq. (A10).

4. Oscillator model

We consider a power grid model consisting of N rotating machines $j \in \{1, \dots, N\}$ representing, for instance, wind turbines, or electric motors [3, 4, 28]. Each machine is characterized by the electric power P_j it generates ($P_j > 0$) or consumes ($P_j < 0$). The state of each machine is determined by its mechanical phase angle $\theta_j(t)$ and its velocity $d\theta_j/dt$. During the regular operation, generators as well as consumers within the grid run with the same frequency $\omega_0 = 2\pi \times 50 \text{ s}^{-1}$ or $\omega_0 = 2\pi \times 60 \text{ s}^{-1}$, respectively. The phase of each element is then written as

$$\theta_j(t) = \omega_0 t + \phi_j(t), \quad (\text{A13})$$

where ϕ_j denotes the phase difference to the reference phase $\omega_0 t$.

The equation of motion for all ϕ_j can now be obtained from energy conservation, that is the generated or consumed energy $P_{\text{source},j}$ of each machine must equal the energy sum given or taken from the grid plus the accumulated and dissipated energy. The dissipation power of each element is given by $P_{\text{diss},j} = \kappa_j(\dot{\theta}_j)^2$, where κ is a friction coefficient. The kinetic energy of a rotating machine with a moment of inertia I_j is given by $E_{\text{kin},j} = I_j \dot{\theta}^2/2$ such that the accumulated power is given by $P_{\text{acc},j} = dE_{\text{kin},j}/dt$. The power transmitted between two machines i and j is proportional to the sine of the relative phase $\sin(\theta_i - \theta_j)$ and the capacity of the respective transmission line $P_{\text{max},ij}$,

$$P_{\text{trans},ij} = P_{\text{max},ij} \sin(\theta_i - \theta_j). \quad (\text{A14})$$

If there is no transmission line between two machines, we have $P_{\text{max},ij} = 0$. The condition of energy conservation

at each node j of the network now reads

$$P_{\text{source},j} = P_{\text{diss},j} + P_{\text{acc},j} + \sum_{i=1}^N P_{\text{trans},ij}. \quad (\text{A15})$$

Note that an energy flow between two elements is only possible if there is a phase difference between these two.

We now insert equation (A13) to obtain the evolution equations for the phase difference ϕ_j . We can assume that phase changes are slow compared to the set frequency, $|\dot{\theta}_j| \ll \omega_0$, such that terms containing $\dot{\phi}_j^2$ and $\dot{\phi}_j\ddot{\phi}_j$ can be neglected. Then one obtains

$$I_j\omega_0\ddot{\phi}_j = P_{\text{source},j} - \kappa_j\omega_0^2 - 2\kappa_j\omega_0\dot{\phi}_j + \sum_{i=1}^N P_{\text{max},ij} \sin(\phi_i - \phi_j). \quad (\text{A16})$$

Note that in the equation only the phase difference ϕ_j to

the reference phase $\omega_0 t$ appears. This shows that only the phase difference between the elements of the grid matters.

For the sake of simplicity we consider similar machines only such that the moment of inertia I_j and the friction coefficient κ_j are the same for all elements of the network. Defining $P_j := (P_{\text{source},j} - \kappa\omega_0^2)/(I\omega_0)$, $\alpha := 2\kappa/I$ and $K_{ij} := P_{\text{max},ij}/(I\omega_0)$ this finally leads to the equation of motion

$$\frac{d^2\phi_j}{dt^2} = P_j - \alpha\frac{d\phi_j}{dt} + \sum_i K_{ij} \sin(\phi_i - \phi_j). \quad (\text{A17})$$

Unless stated otherwise, we assume that all transmission lines are equal, that is

$$K_{ij} = \begin{cases} K & \text{if a link exists between nodes } i \text{ and } j \\ 0 & \text{otherwise.} \end{cases} \quad (\text{A18})$$

-
- [1] E. Katifori, G. J. Szöllösi, and M. O. Magnasco, *Phys. Rev. Lett.* **104**, 048704 (2010).
- [2] R. Albert, H. Jeong, and A. Barabási, *Nature* **406**, 378 (2000).
- [3] P. Kundur, *Power System Stability and Control* (McGraw-Hill, New York, 1994).
- [4] M. Rohden, A. Sorge, M. Timme, and D. Witthaut, *Phys. Rev. Lett.* **109**, 064101 (2012).
- [5] G. Pepermans, J. Driesen, D. Haeseldonckx, R. Belmans, and W. D'haeseleer, *Energy Policy* **33**, 787 (2005).
- [6] J. Carrasco, L. Franquelo, J. Bialasiewicz, E. Galvan, R. Guisado, M. Prats, J. Leon, and N. Moreno-Alfonso, *IEEE Transactions on Industrial Electronics* **53**, 1002 (2006).
- [7] F. Blaabjerg, R. Teodorescu, M. Liserre, and A. Timbus, *IEEE Transactions on Industrial Electronics* **53**, 1398 (2006).
- [8] E. Marris, *Nature* **454**, 570 (2008).
- [9] A. E. Motter and Y.-C. Lai, *Phys. Rev. E* **66**, 065102 (2002).
- [10] M. Schäfer, J. Scholz, and M. Greiner, *Phys. Rev. Lett.* **96**, 108701 (2006).
- [11] I. Z. Kiss, C. G. Rusin, H. Kori, and J. L. Hudson, *Science* **316**, 1886 (2007).
- [12] I. Simonsen, L. Buzna, K. Peters, S. Bornholdt, and D. Helbing, *Phys. Rev. Lett.* **100**, 218701 (2008).
- [13] T. Nishikawa and A. E. Motter, *Proceedings of the National Academy of Sciences* **107**, 10342 (2010).
- [14] S. V. Buldyrev, R. Parshani, G. Paul, H. E. Stanley, and S. Havlin, *Nature* **464**, 1025 (2010).
- [15] A. Vespignani, *Nature Physics* **8**, 32 (2011).
- [16] R. Parshani, S. V. Buldyrev, and S. Havlin, *Proceedings of the National Academy of Sciences* **108**, 1007 (2010).
- [17] P. J. Menck, J. Heitzig, N. Marwan, and J. Kurths, *Nature Physics* **9**, 89 (2013).
- [18] Union for the Coordination of Transmission of Electricity, *Final report on the system disturbance on 4 november 2006*, <http://www.entsoe.eu/~library/publications/ce/otherreports/> (retrieved 13/10/2009) (2007).
- [19] D. Braess, *Unternehmensforschung* **12**, 258 (1968).
- [20] D. Braess, A. Nagurney, and T. Wakolbinger, *Transportation Science* **39**, 446 (2005).
- [21] J. E. Cohen and P. Horowitz, *Nature* **352**, 699 (1991).
- [22] T. Roughgarden and E. Tardos, *J. ACM* **49**, 236 (2002).
- [23] S. Blumsack, L. B. Lave, and M. Ilic, *The Energy Journal* **28**, 73 (2007).
- [24] H. Youn, M. T. Gastner, and H. Jeong, *Phys. Rev. Lett.* **101**, 128701 (2008).
- [25] G. Valiant and T. Roughgarden, *Random Structures and Algorithms* **37**, 495 (2010).
- [26] J. G. Wardrop, *Proc. Inst. Civ. Eng.* **1**, 325 (1952).
- [27] M. J. Beckmann, C. B. McGuire, and C. B. Winsten, *Studies in the Economics of Transportation* (Yale University Press, New Haven, 1956).
- [28] G. Filatrella, A. H. Nielsen, and N. F. Pedersen, *Eur. Phys. J. B* **61**, 485 (2008).
- [29] D. Witthaut and M. Timme, *New J. Phys.* **14**, 083036 (2012).
- [30] A. Nagurney, *EPL* **91**, 48002 (2010).
- [31] J. Grainger and W. Stevenson, *Power System Analysis* (McGraw-Hill, New York, 1994).
- [32] D. Watts and S. H. Strogatz, *Nature* **393**, 440 (1998).
- [33] J. M. Kleinberg, *Nature* **406**, 845 (2000).
- [34] A. L. Barabási and R. Albert, *Science* **286**, 509 (1999).
- [35] S. H. Strogatz, *Nature* **410**, 268 (2001).
- [36] A. Barrat, M. Barthélemy, R. Pastor-Satorras, and A. Vespignani, *Proceedings of the National Academy of Sciences of the United States of America* **101**, 3747 (2004).
- [37] C. M. Schneider, A. A. Moreira, J. S. Andrade, S. Havlin, and H. J. Herrmann, *Proceedings of the National Academy of Sciences* **108**, 3838 (2011).